Journal Pre-proofs

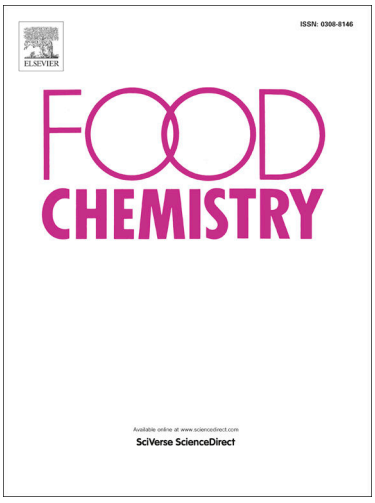

Sensitive electrochemical detection of aflatoxin B1 using DNA tetrahedron-nanostructure as substrate of antibody ordered assembly and template of aniline polymerization

Xiaohui Xiong, Yafei Li, Yichen Lu, Xiong Xiong, Wei Yuan, Yi Li, Yuanjian Liu, Lixia Lu

PII: S0308-8146(20)31230-9
DOI: https://doi.org/10.1016/j.foodchem.2020.127368
Reference: FOCH 127368

To appear in: *Food Chemistry*

Received Date: 11 December 2019
Revised Date: 15 April 2020
Accepted Date: 14 June 2020

Please cite this article as: Xiong, X., Li, Y., Lu, Y., Xiong, X., Yuan, W., Li, Y., Liu, Y., Lu, L., Sensitive electrochemical detection of aflatoxin B1 using DNA tetrahedron-nanostructure as substrate of antibody ordered assembly and template of aniline polymerization, *Food Chemistry* (2020), doi: https://doi.org/10.1016/j.foodchem.2020.127368

Sensitive electrochemical detection of aflatoxin B1 using DNA tetrahedron-nanostructure as substrate of antibody ordered assembly and template of aniline polymerization

Xiaohui Xiong[a], Wei Yuan[a,], Yafei Li[a], Yichen Lu[a], Xiong Xiong[a], Yi Li[a], Yuanjian Liu[a,*], Lixia Lu[a,*]

[a]*Coll Food Sci & Light Ind, Nanjing Tech University, Nanjing 211816, China*

*Corresponding author. Tel.: 86-18795897951; Fax: 86-25-58139527

E-mail address: lucias_cumt@163.com (Y. J. Liu); llxhn66@126.com (L. X. Lu)

Abstract:

A novel strategy for AFB1 detection in grains was proposed based on DNA tetrahedron-structured probe (DTP) and horseradish peroxidase (HRP) triggered polyaniline (PANI) deposition. Briefly, the DNA tetrahedron nanostructures were assembled on the gold electrode, with carboxylic group designed on top vertex of them. The carboxylic group was conjugated with the AFB1 monoclonal antibody (mAb) to form DTP. The test sample and a known fixed concentration of HRP-labeled AFB1 were mixed and they compete for binding to DTP. The HRP assembled on the gold electrode catalyzed the polymerization of aniline on DTP. AFB1 in grains could be determined by using PANI as electrochemical signal molecules. Interestingly, DNA tetrahedron-structure, which has mechanical rigidity and structural stability, can improve antigen-antibody specific recognition and binding efficiency through the use of mAb ordered assembly. Meanwhile, nucleic acid backbone with a large amount of negative charge is good template for aniline polymerization under mild conditions.

Keywords: Electrochemical biosensor; DNA tetrahedral nanostructure; AFB1; PANI; HRP

1. Introduction

Aflatoxin B1 (AFB1) is one of the most chemically toxic known aflatoxins, and agricultural products are deeply affected by it, mainly due to mildew during harvesting and processing (Zhao et al., 2018; Sobolev et al., 2017). The toxicity of AFB1 is mainly manifested in carcinogenesis, mutagenicity, acute toxicity, thermal stability, etc (Chen et al., 2017; Wang, Li, & Zhao, 2019; Qiu et al., 2018; Goud et al., 2018). Therefore, the detection of AFB1 has become particularly important (Myndrul et al., 2017). The current detection methods are UPLC-MS (Romera et al., 2018), fluorescence (Jia et al., 2019; Wang et al., 2016), colorimetric assay (Wu, Zeng, Li, Liu, & Chen, 2019; Lai, Wei, Xu, Zhuang, & Tang, 2017), ELISA, (Xiong et al., 2018; Xiong, Pei, Wu, & Xiong, 2017), and biosensor method (Li et al., 2015) etc. These methods can only be qualitatively judged by fluorescence and colorimetric, while UPLC-MS can be quantified, but the operation is complicated and time-consuming, it is not suitable for quick inspection applications. However, electrochemical biosensors can not only be qualitatively judged, but also can be quantitatively and conveniently operated. Therefore, this study selects electrochemical sensors to detect AFB1 in grains.

How to effectively enhance electrochemical signals by integrating various strategies has been a hot topic. In previous reports, Wang et al. developed a simple signal-on electrochemical sensor, the complementary DNA competed with the modified MB-labeled aptamer on the gold electrode for binding to AFB1 for detection (Wang, Li, & Zhao, 2019). Yu et al. proposed an electrochemical immunosensor that could easily and quickly detect AFB1, and improved the binding efficiency of antigen-antibody by introducing ionic liquid, thereby obtaining higher sensitivity (Yu et al., 2015). Zheng et al. utilized the telomerase amplification to elongate the ssDNA probes on the surface of gold nanoparticles, by which the signal could be correspondingly enlarged (Zheng et al., 2016). In order to improve the sensitivity and stability of electrochemical sensors, some amplification means have been applied in the research. DNA tetrahedron nanostructures have great potential in sensors (Huang, He, & Li, 2018). The rigid structure of DNA tetrahedron nanostructure is relatively stable. It could enhance antigen-binding efficiency through the use of spatially separating pendant probes but also reduces the local overcrowding effect with the overall enhanced packing of targets (Yuan, Giovanni, Xie, Fan, & Leong, 2014; Lu et al., 2019; Wang et al., 2017). Kong et al. established a sensor to improve sensitivity by adjusting the DNA tetrahedron to link HRP to simulate the side length of DNAzyme and GOx at adjacent

vertices (Kong, Wang, Chai, Yuan, & Yuan, 2019). Xie et al. proposed a new application of tetrahedral DNA nanostructures as drug delivery candidate with broad prospects (Xie et al., 2018). Peng et al. demonstrated developed an AFB1 electrochemical aptamer sensor based on tetrahedral DNA nanostructures, which combined tetrahedral DNA nanostructures with AFB1 aptamers and 3DOM MoS_2-AuNPs membranes to construct a sensing interface (Peng et al., 2018).

Meanwhile, DNA tetrahedron nanostructure that have numerous negative charges are good templates for polyaniline (PANI) deposition under mild environment (Zhang, Wang, Zhang, & He, 2018). The PANI formed by the polymerization of aniline is an important conductive polymer possessing reversible redox characteristics, and good stability can be formed by polymerization of aniline under the action of horseradish peroxidase (HRP) or HRP mimic enzyme to amplify the signal (Li, Chang, Hou, & Li, 2016; Wei, & Zhang, 2018). Yukird et al. developed a novel label-free electrochemical immunosensor for the detection of neutrophil gelatinase-associated lipocalcin, which used electropolymerization of aniline to increase the number of amino group used for antibody immobilization (Yukird et al., 2017). Rao et al. proposed a novel molecularly imprinted electrochemical sensor for the detection of melamine. The glassy carbon electrode was modified by gold and polyaniline composite deposited on the surface of glassy carbon electrode to improve electrode sensitivity and amplify sensor signals (Rao et al., 2017). Salahandish et al. proposed a highly sensitive, unlabeled nanometer gene sensor that amplified the signal obtained by polyaniline to detect the known breast cancer biomarker mirna-21 (Salahandish et al., 2018).

In this paper, a rapid and ultrasensitive method for AFB1 detection was designed based on DNA tetrahedron-structured probe (DTP) and HRP triggered PANI deposition. The DNA tetrahedron-structure not only improves antigen-antibody specific recognition and binding efficiency through the use of AFB1 monoclonal antibody (mAb) ordered assembly but also is good template for aniline deposition under mild conditions. Compared with traditional single-stranded DNA probe (ssP), the detection sensitivity was enhanced ~ 100 times by using DTP.

2. Experimental

2.1. Materials and apparatus

All oligonucleotides synthesized and modified used in this experiment by Shanghai Sangon Biological Engineering Technology & Services Co. Ltd (Shanghai, China). The oligonucleotides were showed in Table S1. mAb, HRP-labeled AFB1

(HRP-AFB1), AFB1, Deoxynivalenol (DON), patulin, ochratoxin (OTA), zearalenone (ZEN), AFM1, and AFG1 were purchased from Shanghai Youlong Biotech Co. Ltd (shanghai, China). Aniline, hydrogen peroxide (H_2O_2), N-hydroxysuccinimide (NHS), 1-ethyl-3-(3-dimethylaminopropyl) carbodiimide hydrochloride (EDC), tris (2-carboxyethyl) phosphine hydrochloride (TCEP), 11-mercaptoundecanoic acid (MUA), and 6-Mercapto-1-hexanol (MCH) were purchased from Sigma Aldrich (St Louis, MO, USA). Sample (rice, wheat, corn, sorghum, barley, buckwheat) purchased from a local market in Nanjing, China.

The buffer solutions employed in this study were as follows: 1×PBS (pH 7.2 ~ 7.4, 136.89 mM NaCl, 2.67 mM KCl, 8.24 mM Na_2HPO_4, 1.76 mM NaH_2PO_4); TE buffer (10 mM Tris, pH 8.0, 1 mM EDTA); TM buffer (20 mM Tris, pH 8.0, 50 mM $MgCl_2$); PANI deposition buffer (100 mM acetic acid-sodium acetate (HAc-NaAc), pH 4.3, 200 mM aniline, 20 mM H_2O_2, prepared daily); Electrolyte (100 mM HAc-NaAc buffer, pH 4.3); Electrochemical impedance spectroscopy (EIS) buffer (1×PBS, 5 mM $K_3[Fe(CN)_6]/K_4[Fe(CN)_6]$ (1:1), 100 mM KCl); Ultrapure water (18.2 MΩ cm^{-1} at 25 °C) from a Pure Water system (GWA-UN1-F40, Persee, China) was used in all experiments.

A Model CHI750E Electrochemistry Workstation (Shanghai Chenhua Instruments Co. Ltd., China) was employed for all electrochemical experiments. A conventional three-electrode system was used. A saturated calomel electrode (SCE) and a platinum wire electrode were used as the reference electrode and the auxiliary electrode, respectively. A gold electrode (2 mm in diameter) was used as a working electrode. The morphology of PANI was analyzed using scanning electron microscopy (SEM) system (JEM-2100, JEOL, Japan).

2.2. Synthesis of DNA tetrahedron-structure

The DNA tetrahedron-structure was self-assembled by using methods described in previous reports (Chen et al., 2019; Liu et al., 2016). The four stands (tetra-A-COOH, tetra-B-SH, tetra-C-SH, tetra-D-SH) were used to form DNA tetrahedron-structure. 1 μL of each strand was mixed with 1 μL of TCEP (500 mM) and 45 μL of TM buffer. The resulting mixture was heated to 95 °C for 10 min, and then cooled to 4 °C for 30 min to form DNA tetrahedron-structure.

2.3. Fabrication and Immobilization of DTP on the gold electrode surface

Firstly, the gold electrodes were polished according to the protocol used in a previous work (Zhang, Song, Wang, Pan, & Fan, 2007). Sencondly, 20 μL, 1 μM DNA

tetrahedron-structure was added to gold electrode and incubated overnight at room temperature. Consecutively, a volume of 3 μL of freshly prepared 200 mM EDC and 100 mM EDC were pipetted onto the gold surface and left to react for 15 min. In this way, the carboxylic group on the top of DNA tetrahedron-structure was activated. Finally, after washing with 1×PBS, the activated COOH-terminated electrode was followed by treatment with 20 μL, 100 ng mL^{-1} of the mAb for 2 h at room temperature to obtain DTP sensor.

As a comparison, the single-stranded DNA probe (ssP, SH-T_{10}-COOH) and MUA was immobilized on gold electrode by the same operation. Then, the modified electrode was incubated in 1 mM MCH for 1 h to eliminate nonspecific binding.

2.4. Determination of AFB1 by electrochemical measurements

20 μL of different concentrations of the test sample and 100 ng mL^{-1} HRP-AFB1 were mixed. Then, the mixture solution was dropped on the DTP for 1 h incubation. Part of HRP-AFB1 was assembled on the gold electrode by the antigen-antibody reaction. After washing with 1×PBS, the prepared gold electrode was immersed in 500 μL PANI deposition buffer at the room temperature for 2 h to form PANI. The electrochemical signal was measured with cyclic voltammetry (CV) and differential pulse voltammetry (DPV) by scanning from -0.2 V to 0.2 V in electrolyte. Electrochemical impedance spectroscopy (EIS) was recorded with a frequency range of 0.01 to 10^5 Hz in EIS buffer.

2.5. Real sample treatment

In order to evaluate analytical reliability and application capability of the designed electrochemical biosensor in real samples, rice, wheat, corn, sorghum, barley, buckwheat were selected as model samples to be tested. All samples were purchased from the local market in Nanjing, China. The steps for sample pretreatment were according to the China Food Safety Standard (GB 2761-2017). Firstly, at least 100 g of the sample was weighed and pulverized by a grinder, and the pulverized sample was passed through a 1 mm to 2 mm aperture test sieve. Take 5 g sample in 50 mL centrifuge tube separately, add 25 mL to methanol and water (1:1), shake for 15 min, filter, discard 1/4 initial filtrate and collect sample filtrate, this solution was regard as sample extract. The sample to be tested is diluted with PBS in a sample extract (1:1) to obtain a sample solution.

3. Results and discussion

3.1. Strategy of the AFB1 analysis

In this work, we designed a novel sensor for AFB1 detection in grains based on DTP and HRP triggered PANI deposition. A carboxylic group was designed on top of a DNA tetrahedron-nanostructure, and the mAb for recognition and bind AFB1 specifically could be conjugated on the DNA tetrahedron-nanostructure (Scheme 1) via EDC-NHS method. In this way, a well-controlled antibody monolayer was obtained on the gold electrode surface. A direct competitive enzyme-linked immunoassay was employed in our investigation. After the capture of the mixture of unknown concentration AFB1 and 100 ng mL^{-1} HRP-AFB1, part of HRP was assembled on the gold electrode and employed to catalyze the polymerization of aniline to form PANI, which could be readily detected by using the electrochemical method (Ding et al., 2018; Zhang, Wang, Zhang, & He, 2018; Li, Chang, Hou, & Li, 2016). Interestingly, DNA tetrahedron-structure, which has mechanical rigidity and structural stability, can improve antigen-antibody specific recognition and binding efficiency through the use of mAb ordered assembly. Meanwhile, nucleic acid backbone with a large amount of negative charge is good template for aniline polymerization under mild conditions.

3.2. Characterization of the assembling process

The formation of DNA tetrahedron-nanostructure/gold electrode, DTP/gold electrode, HRP/DTP/gold electrode, and PANI/gold electrode were illustrated by CV and EIS. As the show in Fig. 1A, no CV peak was observed without the deposition of PANI (a, b, c, d in Fig. 1A), while a pair of new redox peaks at -0.089 and -0.019 V appeared due to the redox of PANI (Fig. 1A, e). The appearance of redox peaks demonstrates the successful polymerization of aniline on the electrode surface. Electrontransfer resistance (R_{et}) values also increased stepwise because the negative charges of DNA, antigen and antibody prevent repelling electrons from approaching the electrode surface (a, b, c, d in Fig. 1B). A large decrease in R_{et} was observed (Fig. 1B, e) after the polymerization of PANI because a large amount of conducting PANI enhanced the interfacial electron transfer (Liu et al., 2018; Li, Chang, Hou, & Li, 2016). The surface morphology of formative PANI on the gold electrode surface was characterized by using SEM. As shown in Fig. 1C, the bare gold electrode was smooth and clean. The PANI/gold electrode was granular and rough after polymerization (Fig. 1D). Further study was performed to investigate the scan rate dependence on the response of PANI/gold electrode in electrolyte buffer (Fig. S1). With the rising scan rate, oxidation peak and reduction peak were increased slowly. And the peak responses of the anodic and cathodic about PANI/gold electrode were proportional to the square

root of the scan rate in the range from 20 mV s^{-1} to 500 mV s^{-1}, indicating the DTP sensor was a diffusion controlled process. These results confirmed the formation of PANI on the surface of gold electrode.

3.3. Comparison of different sensing strategies

To verify our hypothesis and to improve the sensitivity, three sensors with different probe were investigated for the analysis of AFB1, including typical small chemical molecule (MUA), single-stranded DNA probe (ssP, SH-T_{10}-COOH), and DTP (this work). The mixture of 10 ng mL^{-1} AFB1 and 100 ng mL^{-1} HRP-AFB1 was used as sample and 100 ng mL^{-1} HRP-AFB1 was analysis as the blank by all three sensors. However, even under the optimal condition, the signal gain of MUA sensor and ssP sensor was almost undetectable, which was probably attributed to the unavoidable cross-masking of binding moieties, they were difficult to maintain stable, unhindered access to the target molecules (Yuan, Giovanni, Xie, Fan, & Leong, 2014; Lu et al., 2019; Wang et al., 2017). Benefiting from the DNA tetrahedron-structure, the DTP sensor achieved lower background and higher signal gain than the other sensors. DNA tetrahedron nanostructure, which has mechanical rigidity and structural stability, can improve antigen-antibody specific recognition and binding efficiency through the use of mAb ordered assembly. Meanwhile, nucleic acid backbone with a large amount of negative charge is good template for aniline polymerization under mild conditions, which also contributed to the high sensitivity. Overall, the results of the DTP sensor investigation were exactly consistent with our prediction.

3.4. Electrochemical analysis of AFB1

Under optimized conditions (Fig. S2), the DTP sensor was used to detect AFB1 and a desirable calibration curve was achieved. Fig. 3A displays the DPV signal corresponding to different concentration of AFB1 in the presence of DTP. The DPV intensity increased monotonically with the logarithm concentration of AFB1 (Fig. 3B, DTP). The dynamic range was from 0.05 to 20 ng mL^{-1}.The detection limit was calculated by $3\sigma_b$/slope (σ_b, standard deviation of the blank samples) to be 0.033 ng mL^{-1}. In contrast, the ssP sensor exhibited a detection limit of 4 ng mL^{-1} AFB1 with the dynamic detection range was from 10 to 60 ng mL^{-1} (Fig. 3B, ssP). Compared with ssP sensor, the sensitivity of DTP sensor was improved ~100 times. Moreover, a comparison of linear ranges and detection limits of other methods as well as the previously reported methods for AFB1 detection is shown in Table S2. This result is better or comparable to most previous reports, and may satisfy the on-site analysis of

AFB1.

3.5. Specificity of the electrochemical biosensor

The specificity of the electrochemical biosensor was further evaluated by analyzing other kinds of mycotoxin including DON, patulin, OTA, ZEN, AFM1, and AFG1. As shown in Fig. 4, an obvious decrease of current intensity was clearly observed in the presence of 10 ng mL^{-1} AFB1 whereas there is no obvious current change with homologous toxins (10 ng mL^{-1} AFM1 and 10 ng mL^{-1} AFG1) and other types of analytes (DON, patulin, OTA, and ZEN) even at 10 times higher concentration than that of AFB1. These results demonstrated that the developed biosensor has sufficient specificity to AFB1 detection.

3.6. Real sample detection

To investigate the feasibility and applicability of the proposed method, the biosensor was used to measure the levels of AFB1 in several real samples. Rice, wheat, corn, sorghum, barley, and buckwheat were selected as model grains to be tested. The experimental results are shown in Table 1. The detection limit of this biosensor (0.05 ng mL^{-1}) is less than the limited values of each model grains in Limit of Fungal Toxins in Food, the National Food Safety Standard of China (GB 2761-2017) (10 ng mL^{-1} for rice, 5 ng mL^{-1} for wheat, 20 ng mL^{-1} for corn, 5 ng mL^{-1} for sorghum, 5 ng mL^{-1} for barley, and 5 ng mL^{-1} for buckwheat). It can be seen from obtained results compared with a commercially available ELISA method that the relative deviation varied from -9.3% to 9.5%, which indicated that there was no obvious difference in between.

4. Conclusions

In summary, a new ultrasensitivity method for the detection of AFB1 in grains was proposed based on DTP and HRP triggered PANI deposition. The DNA tetrahedron nanostructure was conjugated with mAb to form DTP and assembled on the gold electrode. Aniline, catalyzed by HRP and polymerized on the DNA tetrahedron nanostructure, was used to generate excellent electrochemical signals. Particularly, the DNA tetrahedron nanostructure structure endowed the substrate surface with less overcrowding coverage and directly increased the analyte accessibility. The higher rigidity of DTP and its ability can produce uniform and orientational surface assemblies, and improve antigen-antibody specific recognition and binding efficiency. In addition, nucleic acid backbone with a large amount of negative charge is good template for aniline deposition under mild conditions. The proposed electrochemical biosensor exhibited excellent performances in low detection limits and wide linear ranges.

Considering the good biocompatibility and flexible chemical modification of the DTP, this proof-of-concept study of AFB1 detection indicates that this strategy offers a sensitive and promising method for future mycotoxin diagnosis.

Declaration of interests

The authors declare that they have no known competing financial interests or personal relationships that could have appeared to influence the work reported in this paper.

Acknowledgments

This work was financially supported by the National Key Research and Development Program of China (No. 2018YFC1602800), the National Natural Science Foundation of China (No. 21804071), and Natural Science Foundation of Jiangsu Province of China (No. BK20180688).

References

Chen, X., Huang, J., Zhang, S., Mo, F., Su, S., Li, Y., Fang, L., Deng, J., Huang, H., Luo, Z., & Zheng, J. (2019). Electrochemical biosensor for DNA methylation detection through hybridization chain-amplified reaction coupled with a tetrahedral DNA nanostructure. *ACS applied materials & interfaces, 11*(4), 3745-3752. DOI: 10.1021/acsami.8b20144

Chen, X., Che, C., Korolchuk, V. I., Gan, F., Pan, C., & Huang, K. (2017). Selenomethionine alleviates AFB1-induced damage in primary chicken hepatocytes by inhibiting CYP450 1A5 expression via upregulated selw expression. *Journal of agricultural and food chemistry, 65*(12), 2495-2502. DOI: 10.1021/acs.jafc.6b05308

Ding, L., Zhang, L., Yang, H., Liu, H., Ge, S., & Yu, J. (2018). Electrochemical biosensor for p53 gene based on HRP-mimicking DNAzyme-catalyzed deposition of polyaniline coupled with hybridization chain reaction. *Sensors and Actuators B: Chemical, 268,* 210-216. DOI: 10.1016/j.snb.2018.04.126

Goud, K. Y., Kailasa, S. K., Kumar, V., Tsang, Y. F., Gobi, K. V., & Kim, K. H. (2018). Progress on nanostructured electrochemical sensors and their recognition elements for detection of mycotoxins: A review. *Biosensors and Bioelectronics, 121,* 205-222. DOI: 10.1016/j.bios.2018.08.029

Huang, R., He, N., & Li, Z. (2018). Recent progresses in DNA nanostructure-based biosensors for detection of tumor markers. *Biosensors and Bioelectronics, 109,* 27-34. DOI: 10.1016/j.bios.2018.02.053

Jia, Y., Wu, F., Liu, P., Zhou, G., Yu, B., Lou, X., & Xia, F. (2019). A label-free fluorescent aptasensor for the detection of Aflatoxin B1 in food samples using AIEgens and graphene oxide. *Talanta, 198,* 71-77. DOI: 10.1016/j.talanta.2019.01.078

Kong, L., Wang, D., Chai, Y. Q., Yuan, Y., & Yuan, R. (2019). Electrocatalytic efficiency regulation between target-induced HRP-mimicking DNAzyme and GOx with low background for ultrasensitive detection of thrombin. *Analytical chemistry, 91*(15), 10289-10294. DOI: 10.1021/acs.analchem.9b02498

Krittayavathananon, A., & Sawangphruk, M. (2017). Impedimetric sensor of ss-HSDNA/reduced graphene oxide aerogel electrode toward aflatoxin B1 detection: effects of redox mediator charges and hydrodynamic diffusion. *Analytical chemistry, 89*(24), 13283-13289. DOI: org/10.1021/acs.analchem.7b03329

Lai, W., Wei, Q., Xu, M., Zhuang, J., & Tang, D. (2017). Enzyme-controlled dissolution of MnO_2 nanoflakes with enzyme cascade amplification for colorimetric immunoassay. *Biosensors and Bioelectronics, 89,* 645-651. DOI: 10.1016/j.bios.2015.12.035

Li, H., Chang, J., Hou, T., & Li, F. (2016). HRP-mimicking DNAzyme-catalyzed in situ generation of polyaniline to assist signal amplification for ultrasensitive surface plasmon resonance biosensing. *Analytical chemistry, 89*(1)*,* 673-680.

Li, Y., Wen, Y., Wang, L., Liang, W., Xu, L., Ren, S., Zou, Z., Zuo, X., Fan, C., Huang, Q., Liu, G., & Jia, N. (2015). Analysis of telomerase activity based on a spired DNA tetrahedron TS primer. *Biosensors and Bioelectronics, 67,* 364-369. DOI: 10.1016/j.bios.2014.08.056

Liu, Y., Fan, J., Shangguan, L., Liu, Y., Wei, Y., Wei, W., & Liu, S. (2018). Ultrasensitive electrochemical detection of poly (ADP-ribose) polymerase-1 via polyaniline deposition. *Talanta, 180,* 127-132. DOI: 10.1016/j.talanta.2017.11.072

Liu, Y., Wei, M., Liu, X., Wei, W., Zhao, H., Zhang, Y., & Liu, S. (2016). Label-free ultrasensitive detection of telomerase activity via multiple telomeric hemin/G-quadruplex triggered polyaniline deposition and a DNA tetrahedron-structure regulated signal. *Chemical Communications, 52*(9)*,* 1796-1799. DOI: 10.1039/c5cc09800a

Lu, J., Wang, J., Hu, X., Gyimah, E., Yakubu, S., Wang, K., Wu, X., & Zhang, Z. (2019). An electrochemical biosensor based on tetrahedral DNA nanostructures

and G-quadruplex/hemin conformation for the ultrasensitive detection of microRNA-21 in serum. *Analytical chemistry, 9*(11), 7353-7359. DOI: 10.1021/acs.analchem.9b01133

Myndrul, V., Viter, R., Savchuk, M., Koval, M., Starodub, N., Silamiķelis, V., Smyntyna, V., Ramanavicius, A., & Iatsunskyi, I. (2017). Gold coated porous silicon nanocomposite as a substrate for photoluminescence-based immunosensor suitable for the determination of Aflatoxin B1. *Talanta, 175*, 297-304. DOI: 10.1016/j.talanta.2017.07.054

Peng, G., Li, X., Cui, F., Qiu, Q., Chen, X., & Huang, H. (2018). Aflatoxin B1 electrochemical aptasensor based on tetrahedral DNA nanostructures functionalized three dimensionally ordered macroporous MoS_2-AuNPs film. *ACS applied materials & interfaces, 10*(21), 17551-17559. DOI: 10.1021/acsami.8b01693

Qiu, T., Shen, X., Tian, Z., Huang, R., Li, X., Wang, J., Wang, R., Sun, Y., Jiang, Y., Lei, H., & Zhang, H. (2018). IgY reduces AFB1-induced cytotoxicity, cellular dysfunction, and genotoxicity in human L-02 hepatocytes and Swan 71 trophoblasts. *Journal of agricultural and food chemistry, 66*(6), 1543-1550. DOI: 10.1021/acs.jafc.7b05385

Rao, H., Chen, M., Ge, H., Lu, Z., Liu, X., Zou, P., Wang, X., He, H., Zeng, X., & Wang, Y. (2017). A novel electrochemical sensor based on Au@ PANI composites film modified glassy carbon electrode binding molecular imprinting technique for the determination of melamine. *Biosensors and Bioelectronics, 87*, 1029-1035. DOI: 10.1016/j.bios.2016.09.074

Romera, D., Mateo, E. M., Mateo-Castro, R., Gomez, J. V., Gimeno-Adelantado, J. V., & Jimenez, M. (2018). Determination of multiple mycotoxins in feedstuffs by combined use of UPLC–MS/MS and UPLC–QTOF–MS. *Food chemistry, 267,* 140-148. DOI: 10.1016/j.foodchem.2017.11.040

Salahandish, R., Ghaffarinejad, A., Omidinia, E., Zargartalebi, H., Majidzadeh-A, K., Naghib, S. M., & Sanati-Nezhad, A. (2018). Label-free ultrasensitive detection of breast cancer miRNA-21 biomarker employing electrochemical nano-genosensor based on sandwiched AgNPs in PANI and N-doped graphene. *Biosensors and Bioelectronics, 120,* 129-136. DOI: 10.1016/j.bios.2018.08.025

Sobolev, V., Arias, R., Goodman, K., Walk, T., Orner, V., Faustinelli, P., & Massa, A. (2017). Suppression of aflatoxin production in aspergillus species by selected

peanut (Arachis hypogaea) stilbenoids. *Journal of agricultural and food chemistry, 66*(1), 118-126. DOI: 10.1021/acs.jafc.7b04542

Wang, B., Chen, Y., Wu, Y., Weng, B., Liu, Y., Lu, Z., Li, C., & Yu, C. (2016). Aptamer induced assembly of fluorescent nitrogen-doped carbon dots on gold nanoparticles for sensitive detection of AFB1. *Biosensors and Bioelectronics, 78,* 23-30. DOI: 10.1016/j.bios.2015.11.015

Wang, C., Li, Y., & Zhao, Q. (2019). A signal-on electrochemical aptasensor for rapid detection of aflatoxin B1 based on competition with complementary DNA. *Biosensors and Bioelectronics, 144,* 111641. DOI:10.1016/j.bios.2019.111641

Wang, S., Zhang, L., Wan, S., Cansiz, S., Cui, C., Liu, Y., Cai, R., Hong, C., Teng, I. T., Shi, M., Wu, Y., Dong, Y., & Wu, Y. (2017). Aptasensor with expanded nucleotide using DNA nanotetrahedra for electrochemical detection of cancerous exosomes. *ACS nano, 11*(4), 3943-3949. DOI: 10.1021/acsnano.7b00373

Wei, M., & Zhang, W. (2018). Ultrasensitive aptasensor with DNA tetrahedral nanostructure for Ochratoxin A detection based on hemin/G-quadruplex catalyzed polyaniline deposition. *Sensors and Actuators B: Chemical, 276,* 1-7. DOI: 10.1016/j.snb.2018.08.072

Wu, J., Zeng, L., Li, N., Liu, C., & Chen, J. (2019). A wash-free and label-free colorimetric biosensor for naked-eye detection of aflatoxin B1 using G-quadruplex as the signal reporter. *Food Chemistry, 298,* UNSP 125034. DOI: 10.1016/j.foodchem.2019.125034

Xie, X., Shao, X., Ma, W., Zhao, D., Shi, S., Li, Q., & Lin, Y. (2018). Overcoming drug-resistant lung cancer by paclitaxel loaded tetrahedral DNA nanostructures. *Nanoscale, 10*(12), 5457-5465. DOI: 10.1039/c7nr09692e

Xiong, Y., Pei, K., Wu, Y., Duan, H., Lai, W., & Xiong, Y. (2018). Plasmonic ELISA based on enzyme-assisted etching of Au nanorods for the highly sensitive detection of aflatoxin B1 in corn samples. *Sensors and Actuators B: Chemical, 267,* 320-327. DOI: 10.1016/j.snb.2018.04.027

Xiong, Y., Pei, K., Wu, Y., & Xiong, Y. (2017). Colorimetric ELISA based on glucose oxidase-regulated the color of acid–base indicator for sensitive detection of aflatoxin B1 in corn samples. *Food control, 78,* 317-323. DOI: 10.1016/j.foodcont.2017.03.002

Yu, L., Zhang, Y., Hu, C., Wu, H., Yang, Y., Huang, C., & Jia, N. (2015). Highly sensitive electrochemical impedance spectroscopy immunosensor for the

403 detection of AFB1 in olive oil. *Food chemistry, 176,* 22-26. DOI:
404 10.1016/j.foodchem.2014.12.030
405 Yuan, L., Giovanni, M., Xie, J., Fan, C., & Leong, D. T. (2014). Ultrasensitive IgG
406 quantification using DNA nano-pyramids. *NPG Asia Materials, 6*(7), e112. DOI:
407 10.1038/am.2014.46
408 Yukird, J., Wongtangprasert, T., Rangkupan, R., Chailapakul, O., Pisitkun, T., &
409 Rodthongkum, N. (2017). Label-free immunosensor based on
410 graphene/polyaniline nanocomposite for neutrophil gelatinase-associated
411 lipocalin detection. *Biosensors and Bioelectronics, 87,* 249-255. DOI:
412 10.1016/j.bios.2016.08.062
413 Zhang, J., Song, S., Wang, L., Pan, D., & Fan, C. (2007). A gold nanoparticle-based
414 chronocoulometric DNA sensor for amplified detection of DNA. *Nature protocols,*
415 *2*(11), 2888. DOI: 10.1038/nprot.2007.419
416 Zhang, J., Wang, J., Zhang, X., & He, F. (2018). Rapid detection of Escherichia coli
417 based on 16S rDNA nanogap network electrochemical biosensor. *Biosensors and*
418 *Bioelectronics, 118,* 9-15. DOI: 10.1016/j.bios.2018.07.041
419 Zhao, M., Wang, P., Guo, Y., Wang, L., Luo, F., Qiu, B., Guo, L., Su, X., Lin, Z., &
420 Chen, G. (2018). Detection of aflatoxin B1 in food samples based on target-
421 responsive aptamer-cross-linked hydrogel using a handheld pH meter as readout.
422 *Talanta, 176,* 34-39. DOI: 10.1016/j.talanta.2017.08.006
423 Zheng, W., Teng, J., Cheng, L., Ye, Y., Pan, D., Wu, J., Xue, F., Liu, G., & Chen, W.
424 (2016). Hetero-enzyme-based two-round signal amplification strategy for trace
425 detection of aflatoxin B1 using an electrochemical aptasensor. *Biosensors and*
426 *Bioelectronics, 80,* 574-581. DOI: 10.1016/j.bios.2016.01.091

427

Figure captions

Scheme 1 Schematic illustration of AFB1 detection in grains based on DTP and HRP triggered PANI deposition.

Fig. 1 (A) CV and (B) EIS of bare gold electrode (a), DNA tetrahedron-nanostructure/gold electrode (b), DTP/gold electrode (c), HRP/ DTP/gold electrode (d), and PANI/gold electrode (e). SEM images of bare gold electrode (C) and PANI modified gold electrode (D). 10 ng mL^{-1} AFB1 was used.

Fig. 2 AFB1 analysis results from three different sensors: DTP, ssP and MUA. The mixture of 10 ng mL^{-1} AFB1 and 100 ng mL^{-1} HRP-AFB1 was used as sample. 100 ng mL^{-1} HRP-AFB1 was analysis as the blank.

Fig. 3 (A) DPV corresponding to the different AFB1 concentrations using DTP sensor. From a to k: 0.05, 0.1, 0.5, 1, 5, 10, 20, 50, 70, 100, and 150 $ng \cdot mL^{-1}$. (B) The linear plot of DPV current versus the logarithm of AFB1 concentrations ranging from 0.05 $ng \cdot mL^{-1}$ to 20 $ng \cdot mL^{-1}$ using DTP sensor and 10 $ng \cdot mL^{-1}$ to 60 $ng \cdot mL^{-1}$ using ssP sensor. Error bars showed the standard deviation of three experiments.

Fig. 4 Demonstrated selectivity of the electrochemical sensor in the presence of different mycotoxins. Error bars showed the standard deviation of three experiments.

Table 1. Recoveries of AFB1 in grain samples for applicability of biosensor and the ELISA kit. College of chemistry and pharmaceutical sciences

453 **Scheme 1**

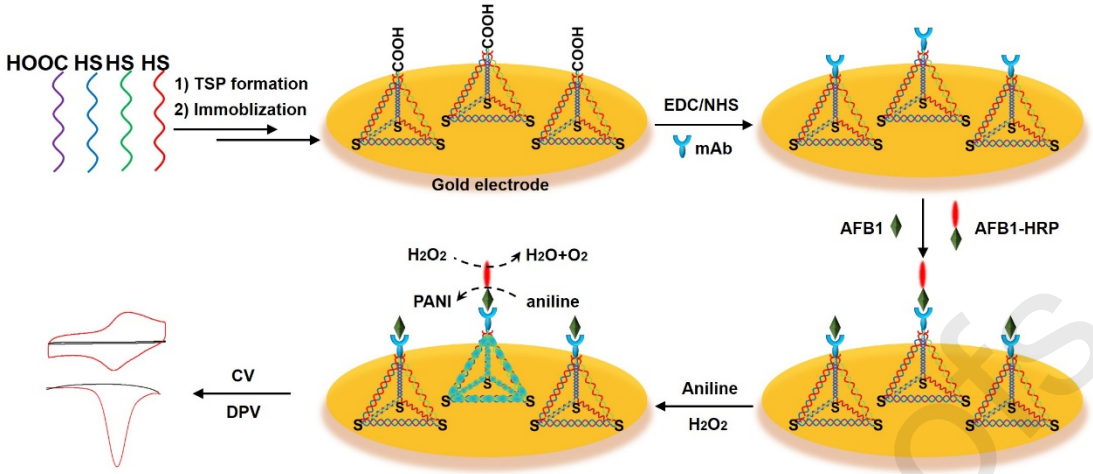

454

455

456

Fig. 1

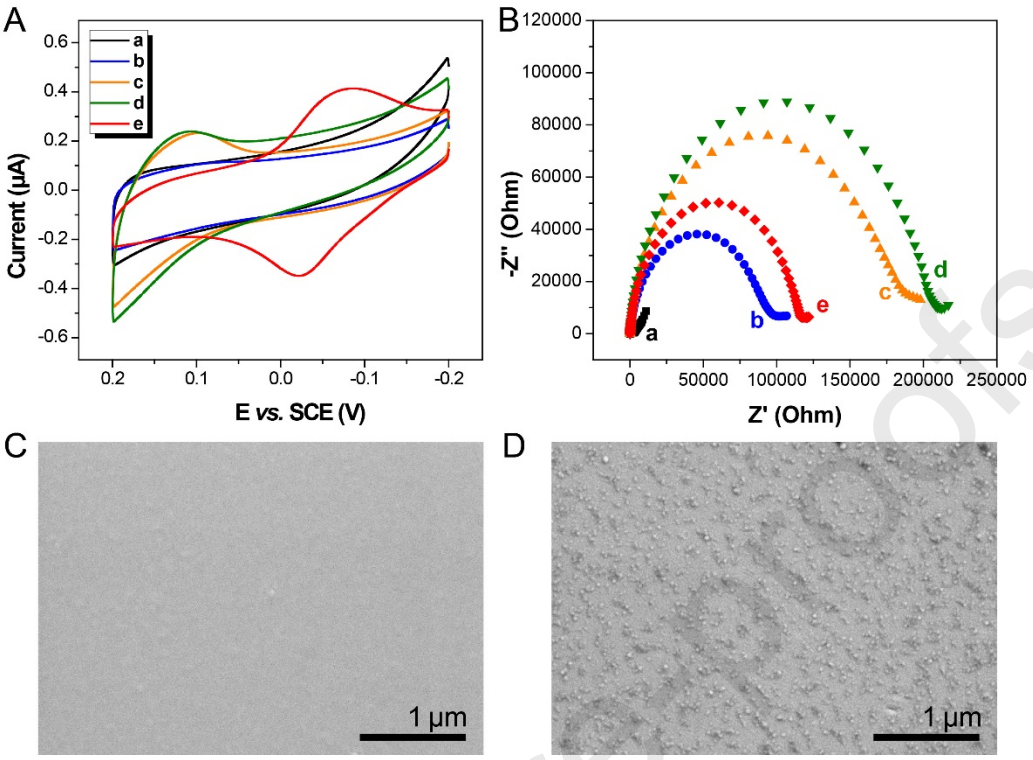

457

458

459 **Fig. 2**

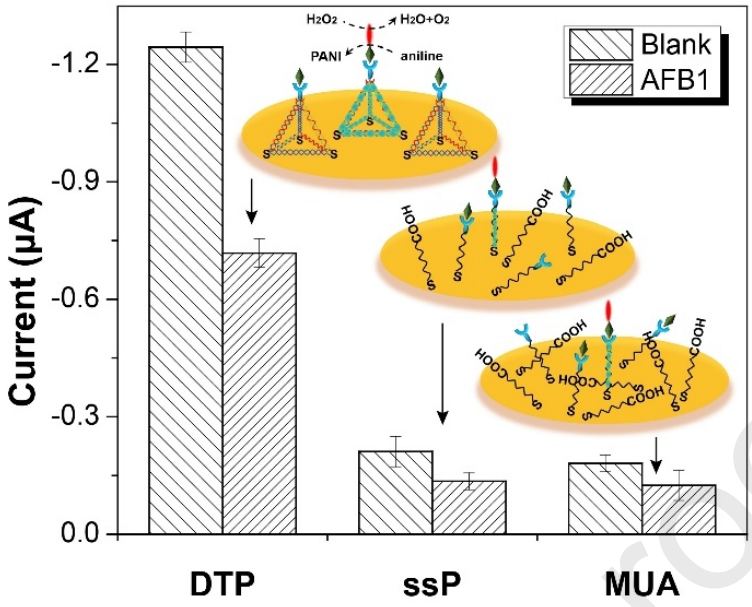

460

461

462 **Fig. 3**

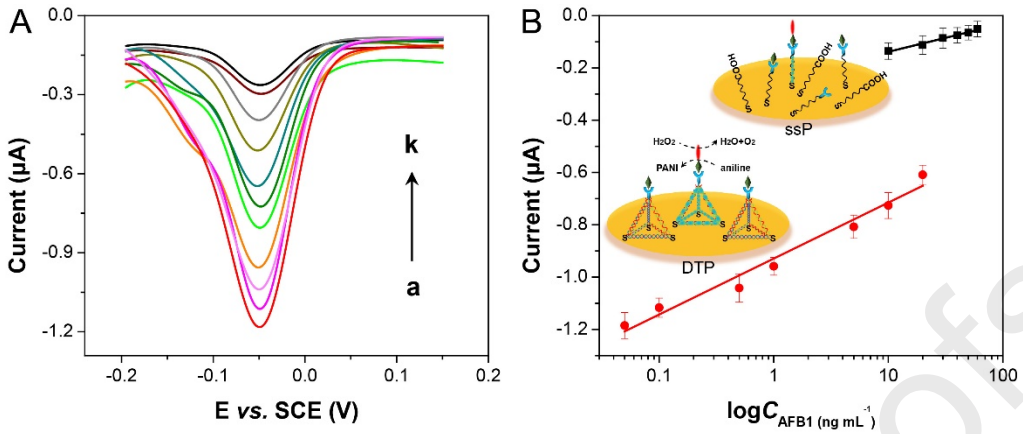

463

464

465 **Fig. 4**

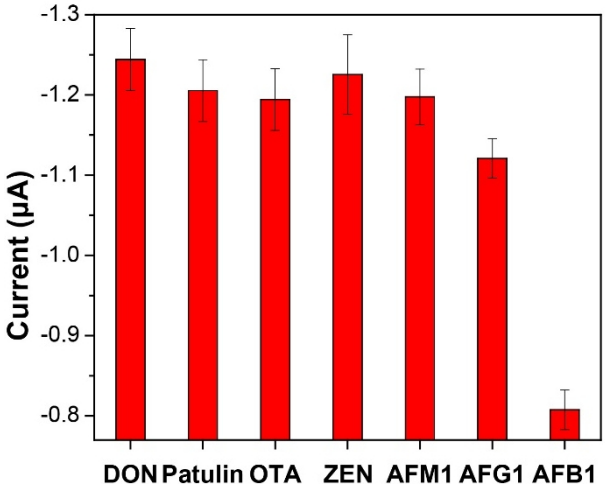

466

467

Table 1
Recoveries of AFB1 in grain samples for applicability of biosensor and the ELISA kit.

Sample	Original (ng mL^{-1})	Added[a] (ng mL^{-1})	Found[b] (ng mL^{-1})		Relative deviation (%)
			ELISA	Biosensor	
Rice	0	1.0	0.89	0.94	-5.6
		10	9.8	9.6	2.0
		20	21	19	9.5
Wheat	0	0.50	0.53	0.52	1.9
		5.0	4.8	4.6	4.2
		10	9.2	9.8	-6.5
Corn	0	2.0	1.9	1.8	5.3
		20	19	20	-5.3
		50	46	47	-2.2
Sorghum	0	0.50	0.43	0.47	-9.3
		5.0	4.6	4.5	2.2
		10	9.6	9.7	-1.0
Barley	0	0.50	0.47	0.51	-8.5
		5.0	4.5	4.9	-8.9
		10	9.6	9.3	3.1
Buckwheat	0	0.50	0.52	0.48	7.7
		5.0	4.7	4.5	4.3
		10	9.0	9.7	-7.8

[a]The bold italic data are the limited values of each grain samples in Limit of Fungal Toxins in Food, the National Food Safety Standard of China (GB 2761-2017).
[b]Each data point present an average of five independent measurements.

Wei Yuan and Xiong Xiong: Data curation, Writing - original draft. Yafei Li and Yichen Lu: Conceptualization, Methodology, Writing - review & editing. Xiaohui Xiong and Yuanjian Liu: Funding acquisition, Project administration, Writing - review & editing. Lixia Lu and Yi Li: Formal analysis, Software, Supervision.

Declaration of interests

☑The authors declare that they have no known competing financial interests or personal relationships that could have appeared to influence the work reported in this paper.

☐The authors declare the following financial interests/personal relationships which may be considered as potential competing interests:

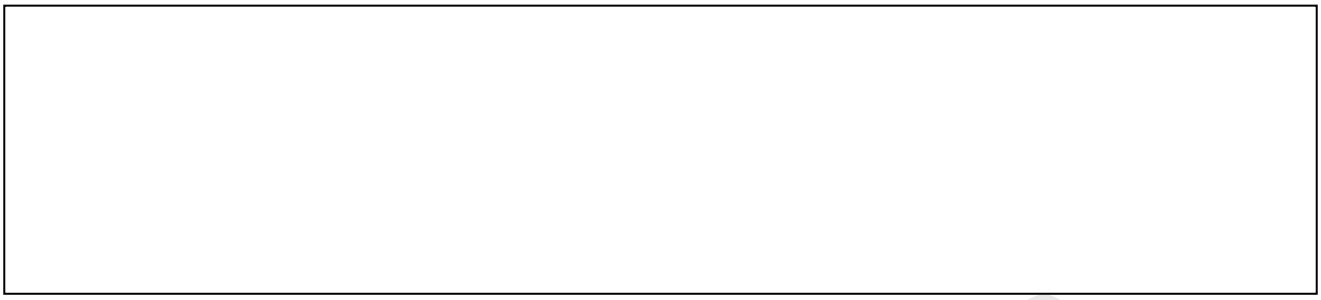

A strategy for detection of AFB1 based on DTP sensor

The DTP can improve antigen-antibody specific recognition and binding efficiency

The DTP is good template for aniline polymerization under mild conditions